Microporous and Mesoporous Materials 167 (2013) 44–50

Contents lists available at SciVerse ScienceDirect

Microporous and Mesoporous Materials

journal homepage: www.elsevier.com/locate/micromeso

MgO-modified mesoporous silicas impregnated by potassium carbonate for carbon dioxide adsorption

Arnošt Zukal, Jakub Pastva, Jiří Čejka *

J. Heyrovský Institute of Physical Chemistry, Academy of Sciences of the Czech Republic, v.v.i., Dolejškova 3, 18223 Prague 8, Czech Republic

ARTICLE INFO

Article history:
Available online 29 May 2012

Dedicated to Prof. Carmine Colella on the occasion of his 70th birthday.

Keywords:
Mesoporous adsorbents
SBA-15 silica
Introducing of MgO and K_2CO_3
Adsorption of CO_2

ABSTRACT

Mesoporous adsorbents for carbon dioxide capture were prepared by introducing of magnesium oxide and potassium carbonate into SBA-15, SBA-16 silicas and MCM-48-like-silica. In order to avoid destruction of silica supports, a novel procedure based on the precipitation of magnesium acetate on the silica surface was developed. Subsequent *in situ* chemical conversion of magnesium acetate provided magnesium oxalate, while final magnesium oxide was formed by calcination. To introduce potassium carbonate, silica modified with MgO was impregnated with potassium oxalate followed by its conversion to carbonate. All prepared mesoporous adsorbents preserved characteristic features of mesoporous molecular sieve.

The comparison of carbon dioxide isotherms obtained on prepared samples reveals that their adsorption properties are decisively influenced by the type of mesoporous structure. Modified sample of SBA-15 silica has shown the most steep adsorption isotherm and higher CO_2 adsorption capacity than adsorption capacity of samples prepared from SBA-16 and MCM-48-ls silicas.

1. Introduction

Capture and storage of carbon dioxide is one of the most challenging issues in the field of material science and adsorption [1–4]. In the case of physical adsorption of CO_2, nanoporous materials are primarily investigated, including alkali-metal exchanged zeolites [5–13], amino-modified [14–22] and alkali-modified [23] mesoporous silicas, and recently also metal–organic frameworks [24–26] or organo-modified mesoporous silicas [27]. These adsorbents differ from each other based on their chemical composition, structure and type of adsorption sites and also adsorption enthalpy. In addition to numerous experimental contributions, theoretical contributions were particularly efficient, *e.g.* in analyzing high adsorption enthalpy at low coverage for Na-FER zeolites. DFT calculations allowed for understanding of the formation of "dual sites", in which CO_2 molecule bridges two alkali metal cations [9,12]. The MIL series of metal–organic frameworks [28] are promising candidates for the purpose of CO_2 adsorption. Enthalpies of CO_2 adsorption at low coverage in the different pore versions of MIL-53 (Al) were predicted using grand canonical Monte Carlo simulations [29].

Among alkaline earth metal oxides mesoporous magnesium oxide has been studied as a plausible CO_2 adsorbent mainly because of its lower energy requirements for regeneration [1]. In general, synthesis processes for mesoporous MgO are time consuming, involve multistep procedures, use a template and/or need toxic solvents (see reviews [1,3,4]). For example, Roggenbuck et al. prepared periodically ordered mesoporous magnesium oxide [30,31]; however, complicated double replication procedure was used. As for adsorption purposes perfectly ordered materials are not needed, simple synthesis procedures yielding stable MgO of high surface area remain popular [32]. To prepare magnesium oxide of small particles exposing more adsorption centers into the gas phase, we have focused on introduction of MgO into mesoporous molecular sieves benefiting from thermal stability and large surface area of mesoporous silicas. In our previous study we have shown that potassium cations in Al-SBA-15 dramatically enhance adsorption of CO_2 in the region of low equilibrium pressures [22].

In current contribution we have promoted magnesium oxide containing mesoporous silicas with potassium carbonate. For that purpose, a novel procedure of the preparation of mesoporous Mg-SBA-15 adsorbent with further introduction of potassium cations was developed. CO_2 adsorption isotherms were recorded in the temperature range between 0 and 60 °C to achieve isosteric heats of CO_2 adsorption on Mg/K-SBA-15. Finally, isosteric heats are discussed in a view of other nanoporous adsorbents.

2. Experimental

2.1. Materials

All chemicals used were obtained from Sigma–Aldrich and used as supplied. Starting mesoporous silicas SBA-15, SBA-16 and

* Corresponding author. Tel.: +420 26605 3795; fax: +420 28658 2307.
E-mail address: jiri.cejka@jh-inst.cas.cz (J. Čejka).

1387-1811/$ - see front matter © 2012 Elsevier Inc. All rights reserved.
http://dx.doi.org/10.1016/j.micromeso.2012.05.026

MCM-48-like silica (denoted here as MCM-48-ls) were synthesized according to the methods reported in references [33–35], respectively. Tetraethyl orthosilicate (TEOS) was used as silica source; amphiphilic triblock copolymers poly(ethylene oxide)-poly(propylene oxide)-poly(ethylene oxide) P123 and F127 were applied as structure directing agents. Syntheses of SBA-15 and SBA-16 were performed in diluted solution of hydrochloric acid at 95 °C for 72 h. The molar compositions of the reaction mixture for the synthesis of SBA-15 was 1 TEOS: 0.017 P123: 6.1 HCl: 197 H_2O while SBA-16 was synthesized using the reaction mixture having the molar composition 1 TEOS: 0.0025 P123: 0.0034 F127: 4.9 HCl: 150 H_2O. The synthesis of MCM-48-ls was carried out using n-butanol (BuOH) as a co-solvent. The molar composition of the synthesis mixture was 1 TEOS: 0.017 P123: 1.82 HCl: 195 H_2O: 1.31 BuOH. This mixture was prepared at 35 °C and aged at 100 °C under static conditions for 48 h. The resulting solid was recovered by filtration, extensively washed with distilled water and ethanol, and dried at 95 °C overnight. The template was removed by calcinations in air at 540 °C for 8 h (temperature ramp of 1 °C/min).

MgO-modified materials were prepared by precipitation of magnesium acetate on the silica surface followed by subsequent chemical conversion. In order to prepare these samples, 2 g of the respective silica support were added to solution of 5 ml of ethanol and 5 ml of distilled water containing 2 g of magnesium acetate tetrahydrate. After stirring for 5 min. the solid phase was separated by vacuum filtration and dried at 75 and 115 °C always for 1 h. After that it was soaked in 10 ml of ethanolic solution of oxalic acid (30 g of oxalic acid in 100 ml of ethanol) for 10 min. The powder was filtered, dried at 75 °C and calcined in air at 300 °C for 10 h (temperature ramp of 1 °C/min).

In order to enhance carbon dioxide adsorption, magnesium oxide containing samples were modified with potassium carbonate. For that purpose 0.5 g of sample was soaked in 3 ml of 0.5 M potassium oxalate aqueous solution. Samples were dried in vacuum at ambient temperature for 12 h. To form potassium carbonate, calcination was carried out in air at 300 °C for 6 h (temperature ramp of 1 °C/min).

All samples under study are listed in Table 1. The samples are labeled as SBA-15, Mg-SBA-15, Mg/K-SBA-15 *etc.*

2.2. Methods

X-ray powder diffraction data were recorded on a Bruker D8 X-ray powder diffractometer equipped with a graphite monochromator and a position-sensitive detector (Våntec-1) using Cu Kα radiation (at 40 kV and 30 mA) in Bragg–Brentano geometry.

Adsorption isotherms of nitrogen at −196 °C (*i.e.* 77.35 K) and carbon dioxide at 0–60 °C on materials under study were determined using an ASAP 2020 (Micromeritics) volumetric instrument. The instrument was equipped with three pressure transducers covering 133 Pa, 1.33 kPa and 133 kPa ranges. To avoid potential structural damage of the sample, all the materials were outgassed before adsorption measurement using a program starting from ambient temperature to 110 °C (heating ramp of 0.5 °C/min) until the residual pressure of 1 Pa was reached. After 1 h delay at 110 °C the temperature was further increased (heating ramp of 1 °C/min) to 300 °C. The sample was outgassed at this temperature under turbomolecular pump vacuum for 8 h.

The Iso-Therm thermostat (e-Lab Services, Czech Republic) maintaining temperature of the sample with accuracy of ±0.01 °C was used for the measurement of carbon dioxide adsorption at 0, 20, 40, and 60 °C. (The exact temperature of each measurement was determined using platinum resistance thermometer.) As adsorption isotherms of carbon dioxide were measured on the same sample immediately after nitrogen adsorption measurement, the degas procedure was performed at 300 °C for 8 h under turbomolecular pump vacuum. These conditions were also applied when carbon dioxide adsorption measurement was repeated at another temperature.

The composition of samples prepared was determined by means of standard analytical methods. The magnesium content was estimated titrimetrically after dissolution of analyzed sample in a mixture of hydrofluoric and perchloric acids. The amount of potassium cations was determined by using atomic absorption spectroscopy ZEEnit 700 (Analytik Jena, Germany.) The measurements were carried out with flame atomization, and Deuterium lamp was used as background correction. The resonance lines of hollow cathode lamps (HCl, Analytik Jena, Germany) were used for the study of element. Obtained results expressed in miligram of MgO and K_2CO_3 per 1 g of silica are given in Table 1.

3. Results and discussion

3.1. Preparation of adsorbents

The application of common synthesis procedures such as impregnation with solutions of magnesium acetate, magnesium nitrate, sodium or potassium carbonate or bicarbonate was unsuccessful and led to a collapse of the mesoporous system observed after drying and calcination of sample. (Nitrogen isotherm on SBA-15 treated with potassium bicarbonate shown in Supporting information illustrates a collapse of the original porous structure.) In order to introduce magnesium oxide or alkali metal carbonate on the inner surface of mesoporous silica without destruction of the parent porous system, a special method was developed. This procedure, similar to the template synthesis of macroporous solids suggested by Stein et al. [36], is based on the precipitation of metal salts on the mesoporous silica surface and subsequent chemical

Table 1
Physicochemical properties of adsorbents for CO_2.

Sample code	MgO (mg/g)	K_2CO_3 (mg/g)	S_{BET} (m^2/g)	V_{ME} (cm3/g)	D_{ME} (nm)	a_{10}[a] (cm^3/g) STP	a_{100}[b] (cm^3/g) STP
SBA-15	–	–	660	1.03	10.2	2.0	16.5
Mg-SBA-15	38	–	464	0.65	9.2	1.7	12.2
Mg/K-SBA-15	38	43	257	0.49	8.7	7.8	18.8
SBA-16	–	–	710	0.53	7.7	2.5	20.6
Mg-SBA-16	20	–	489	0.41	7.4	3.0	16.6
Mg/K-SBA-16	20	27	273	0.27	7.1	2.9	10.3
MCM-48-ls	–	–	867	1.06	11.1	2.5	20.1
Mg-MCM-48-ls	39	–	530	0.74	10.7	3.2	16.7
Mg/K-MCM-48-ls	39	49	318	0.52	10.1	3.7	12.7

[a] Amount adsorbed at 10 kPa and 20 °C.
[b] Amount adsorbed at 100 kPa and 20 °C.

conversion of the inorganic precursor. It is well-known that magnesium oxalate decomposes directly before melting to form magnesium oxide. Because magnesium oxalate is insoluble in water or ethanol, we performed *in situ* chemical reaction by introducing solution of oxalic acid into the silica containing magnesium acetate. Similarly, we introduced potassium carbonate into silica pores: MgO/silica was impregnated with potassium oxalate solution followed by its conversion to carbonate. As stated *vide supra*, this method was not successful for modification of pure silica supports.

3.2. Porous structure of samples

Nitrogen adsorption isotherms for parent samples of SBA-15, SBA-16 and MCM-48-ls (Figs. 1–3, respectively) are materials with mesoporous character according to the IUPAC classification. The isotherms on SBA-15 and MCM-48-ls featured hysteresis loops with sharp adsorption/desorption branches at relative pressure p/p_0 of 0.68/0.75 and 0.70/0.77, respectively. The steepness of both adsorption and desorption branches is indicative of a narrow mesopore size distribution. The adsorption isotherm on SBA-16 has hysteresis loop of type H2 according to the IUPAC classification with steep desorption branch at p/p_0 of 0.45. This type of hysteresis loop is characteristic of mesoporous materials with narrow pore entrances.

Table 1 lists textural data of parent and modified samples under study. The BET surface area S_{BET} was evaluated using adsorption data in a relative pressure range from 0.05 to 0.25. Therefore, the parent materials contain only a negligible amount of micropores. The mesopore volume and mesopore size distributions of the SBA-15, SBA-16 and MCM-48-ls were evaluated by means of the NLDFT using the Micromeritics software and kernel for nitrogen, cylindrical pores and oxide surface. (This kernel is not strictly adequate for application to SBA-16 and MCM-48-ls materials. On the other side, according to our opinion, this model is better than kernel for slit-shaped pores.) Obtained mean diameter of cylindrical mesopores of SBA-15 is 10.2 nm. Three-dimensional cubic mesostructure of MCM-48-Is consists of two interpenetrating networks of chiral channels [31] with a mean diameter about 11.1 nm. The

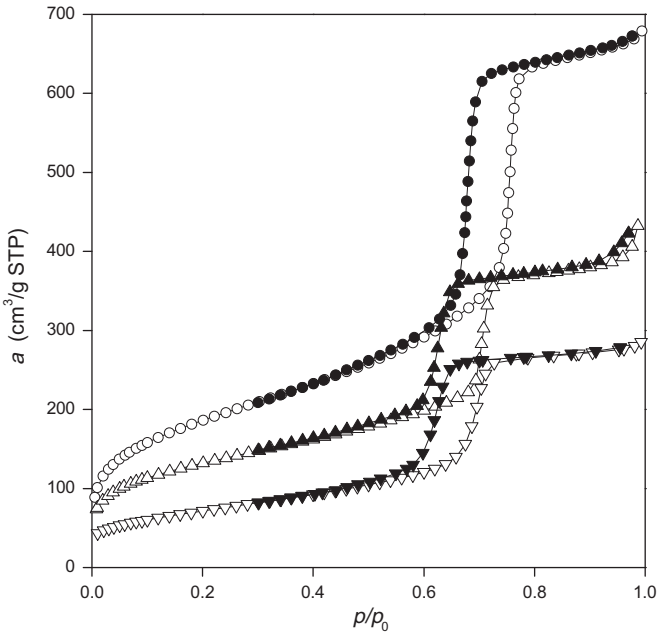

Fig. 1. Nitrogen adsorption isotherms on SBA-15 (○), Mg-SBA-15 (△) and Mg/K-SBA-15 (▽) at −196 °C. (Solid points denote desorption.)

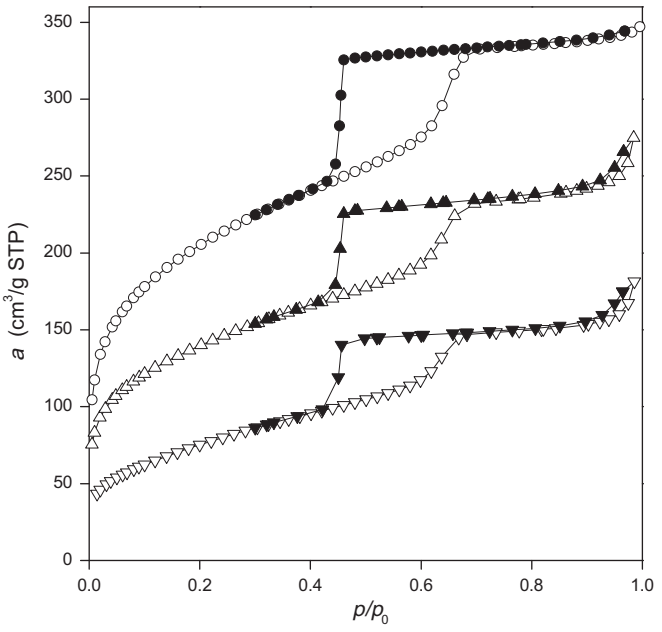

Fig. 2. Nitrogen adsorption isotherms on SBA-16 (○), Mg-SBA-16 (△) and Mg/K-SBA-16 (▽) at −196 °C. (Solid points denote desorption.)

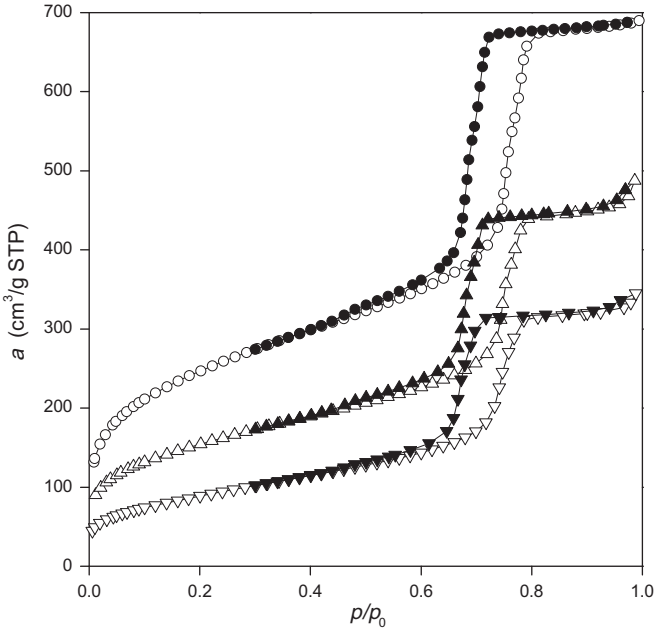

Fig. 3. Nitrogen adsorption isotherms on MCM-48-ls (○), Mg-MCM-48-ls (△) and Mg/K-MCM-48-ls (▽) at −196 °C. (Solid points denote desorption.)

cubic mesostructure of SBA-16 is composed from spherical cages, each of them having eight entrances [30]. Obtained diameter of cages is 7.7 nm.

As template was removed from the as-synthesized samples by calcination, some shrinkage of the silica pore walls occurred, as reported earlier [37]. It was shown [32] that the template removal from the as-synthesized material at temperatures higher than 540 °C facilitates the shrinkage leading to the strong decrease in the micropore volume ("surface roughness".) In accordance with this observation, an application of the *t*-method has revealed that the microporosity of our samples is negligible. (The Kruk-Jaroniec-Sayari

thickness equation was used as the reference isotherm. The *t*-plots are displayed in Supporting Information, Fig. SI 3.)

To examine the influence of grafting with magnesium oxide and the presence of potassium carbonate in the pores, nitrogen isotherms were measured on modified samples. Figs. 1–3 show nitrogen isotherms of parent and grafted silicas. The surface area S_{BET}, mesopore volume V_{ME} and mesopore diameter D_{ME} of the parent and modified samples are summarized in Table 1.

The inspection of nitrogen isotherms reveals that the structural features of all three silica types are preserved after the introduction of MgO and K_2CO_3. (This fact is also confirmed by X-ray diffraction shown in Supporting Information, Fig. SI 1). Surface area S_{BET} and mesopore volume V_{ME} decreased significantly upon the introduction of MgO and K_2CO_3; a slight decrease was found also for the mesopore diameters D_{ME}.

The decrease in the pore volume and surface area due to post-synthesis modifications of parent silicas is not proportional to the mass of deposited compounds .With respect to the relatively small mass of deposited compounds, the reduction of textural parameters would be much lower if these compounds would be located exclusively on the external surface of the particles. The strong reduction of texture parameters indicates that deposited compounds are located inside the particles.

The mentioned changes in the textural parameters are similar to those observed with grafting of alumina on SBA-15 [32]. Although complete explanation was not suggested yet, it is obvious that the smoothing of the mesopore surface can play important role. We have shown in Ref. [38] that the mesopores of the SBA-15 silica are surrounded by a corona due to the roughness of their surface. The filling of corona with aluminum oxide results in a gradual smoothing of the surface and leads to a decrease in surface area. Similar effect can be expected when introducing MgO into SBA-15 silicas.

3.3. Adsorption of carbon dioxide

Adsorption isotherms of carbon dioxide at 20 °C for samples under study are displayed in Figs. 4–6. The isotherms on parent silicas SBA-15, SBA-16 and MCM-48-ls are almost linear and they reveal that pure silica does not interact very strongly with CO_2 because the surface hydroxyl groups are not able to induce sufficiently strong interactions and other adsorption sites are missing. The weak interaction of CO_2 with surface of Al-SBA-15 silica was also reported [22]. In addition, the size of the pores is too large to influence the adsorption by the effect "from the top" as recently described by Nachtigall et al. [39,40] and which is so important in the case of CO_2 adsorption in microporous zeolites. The CO_2 isotherms on modified samples exhibit nonlinear concave decreasing course typical for adsorption of CO_2 on inorganic materials (zeolites, mesoporous adsorbents, hydrotalcite-like compounds.) The steepness of these isotherms and the CO_2 adsorption capacity are characterized by the amounts a_{10} and a_{100} adsorbed at 10 and 100 kPa, respectively (Table 1). As follows from the presented data, these adsorption characteristics depend on both the type of silica support and the introduction of potassium carbonate. It is evident that the sample Mg/K-SBA-15 is characterized by the very steep adsorption isotherm and the highest adsorption capacity at a pressure of 100 kPa. Amounts of CO_2 adsorbed a_{10} and a_{100} for the sample Mg-SBA-15 are equal only to 1.7 cm^3/g STP and 12.2 cm^3/g STP, respectively. However, after the promotion with K_2CO_3 they increase to 7.8 cm^3/g STP and 18.8 cm^3/g STP, respectively. Although the samples Mg/K-SBA-15 and Mg/K-MCM-48-ls contain practically the same amounts of MgO and K_2CO_3, the amounts adsorbed a_{10} and a_{100} for Mg/K-MCM-48-ls are equal to only 3.7 cm^3/g STP and 12.7 cm^3/g STP, respectively. The mesopore volume of the support SBA-16 is smaller than mesopore volume of SBA-15

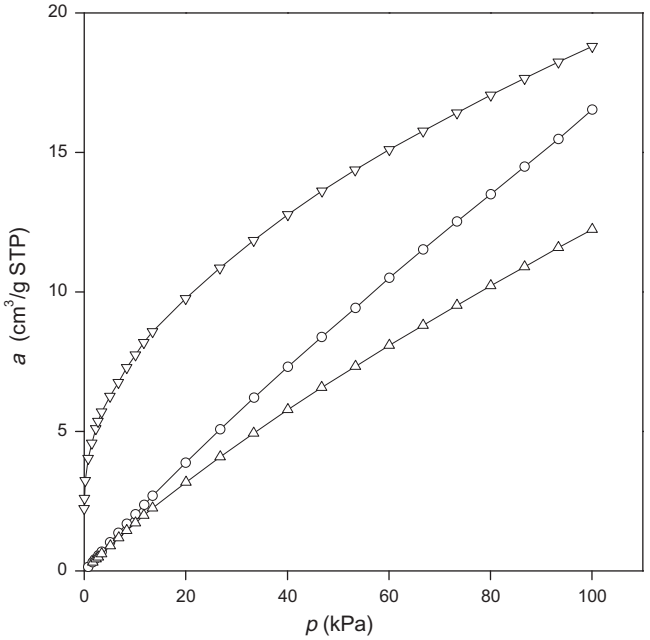

Fig. 4. Adsorption isotherms of carbon dioxide on SBA-15 (○), Mg-SBA-15 (△) and Mg/K-SBA-15 (▽) at 20 °C.

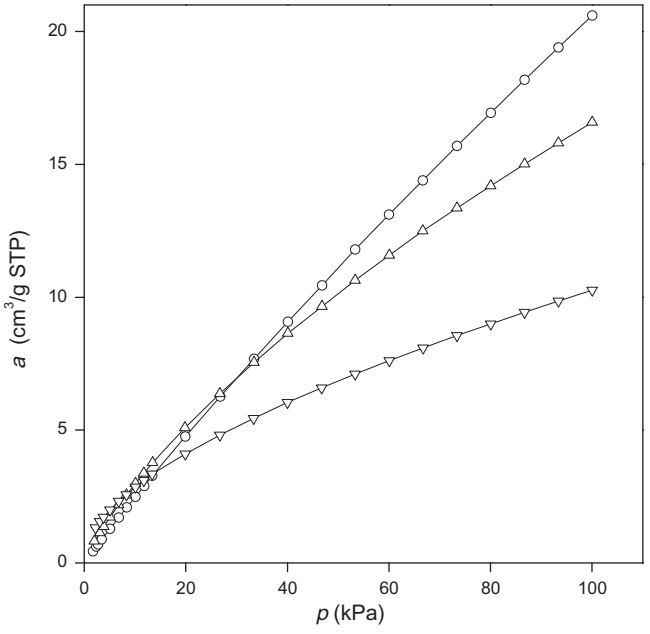

Fig. 5. Adsorption isotherms of carbon dioxide on SBA-16 (○), Mg-SBA-16 (△) and Mg/K-SBA-16 (▽) at 20 °C.

and MCM-48-ls. Therefore, due to a smaller volume of impregnation solution soaked into the mesopores the sample Mg/K-SBA-16 contains less MgO and K_2CO_3 than samples Mg/K-SBA-15 and Mg/K-MCM-48-ls; its adsorption characteristics are comparable with those of Mg/K-MCM-48-ls.

Magnesium oxide based adsorbents promoted with potassium carbonate have been recently prepared and studied in detail [41]. However, the mechanism of CO_2 capture and the role of K_2CO_3 have not been clearly defined. SBA-16 and MCM-48-ls provide highly opened porous materials for guest species. It can be supposed that in the cage-like porous structure Mg/K-SBA-16 particles

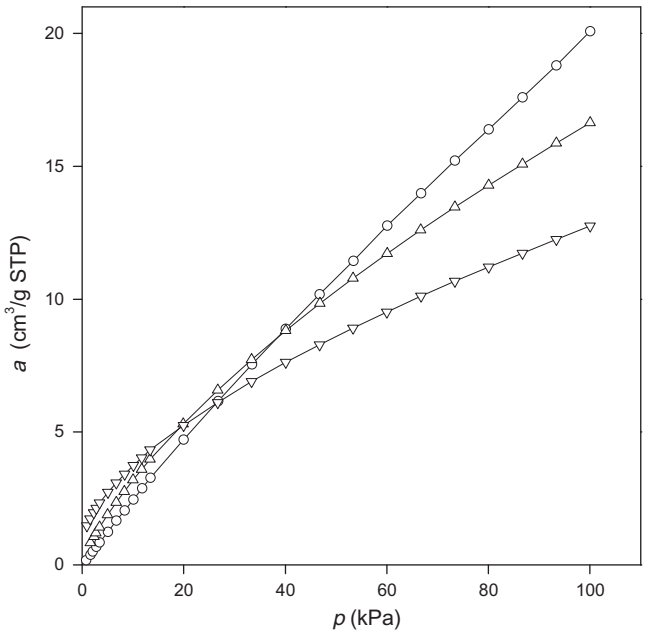

Fig. 6. Adsorption isotherms of carbon dioxide on MCM-48-ls (○), Mg-MCM-48-ls (△) and Mg/K-MCM-48-ls (▽) at 20 °C.

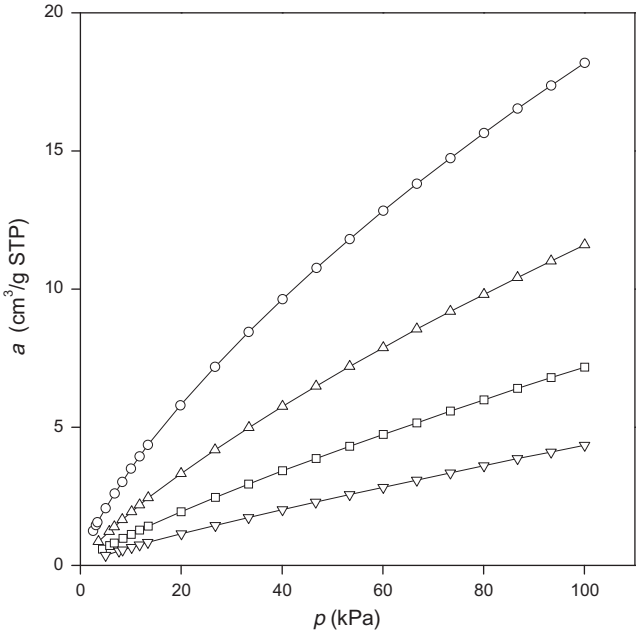

Fig. 7. Carbon dioxide isotherms on Mg-SBA-15 at 0 °C (○), 20 °C (△), 40 °C (□) and 60 °C (▽).

of MgO and K_2CO_3 are formed, which are larger than the same particles in Mg/K-SBA-15. Similar effect can take place in the open porous structure of Mg/K-MCM-48-ls. Due to the smaller surface area of larger MgO and K_2CO_3 particles less active centers is exposed to carbon dioxide molecules. Therefore, adsorption characteristics a_{10} and a_{100} of Mg/K-SBA-16 and Mg/K-MCM-48-ls are lower than those of Mg/K-SBA-15.

It can be summarized that adsorbent based on the SBA-15 silica shows adsorption capacity higher than adsorbents based on SBA-16 or MCM-48-ls. Due to steep adsorption isotherm the sample Mg/K-SBA-15 can be suitable for the carbon dioxide separation from dilute gas mixtures. This behavior of Mg/K-SBA-15 is similar to amine-modified SBA-15 materials, which also exhibit high adsorption enthalpies at low CO_2 coverage [21]. With respect to the properties of Mg-SBA-15 and Mg/K-SBA-15 adsorption isotherms of carbon dioxide in the temperature range from 0 to 60 °C were measured (Figs. 7 and 8). In general, the adsorbed amounts of CO_2 decrease with increasing adsorption temperatures for all samples studied. The temperature dependence of CO_2 adsorption enables us to determine the isosteric adsorption heat Q_{st}. Adsorption isosteres were calculated from isotherms using a polynomial interpolation procedure in coordinates log$p$ vs. a. (With some isotherms a very short polynomial extrapolation was performed.) The sets of adsorption isosteres of CO_2 on Mg-SBA-15 and Mg/K-SBA-15 in coordinates log$p$ vs. $10^3/T$ are shown in Figs. 9 and 10. As all isosteres are linear, isosteric adsorption heat does not depend on temperature.

The isosteric heat of adsorption, Q_{st}, was determined from Clausius–Clapeyron equation:

$$[\partial(\log p)/\partial(1/T)]_a = -Q_{st}/2.303R, \quad (1)$$

where R is the gas constant. Dependences of isosteric adsorption heats Q_{st} on the amount of CO_2 adsorbed are presented in Fig. 11. Low values of Q_{st} for SBA-15 and Mg-SBA-15 indicate a weak interaction of CO_2 molecule with the materials without potassium cations. The weak interaction of CO_2 with MgO is well-known property of this oxide and it makes lower energy requirements for regeneration [1]. However, due to relatively small adsorption capacity pure magnesium oxide is not a strong option for CO_2 capture.

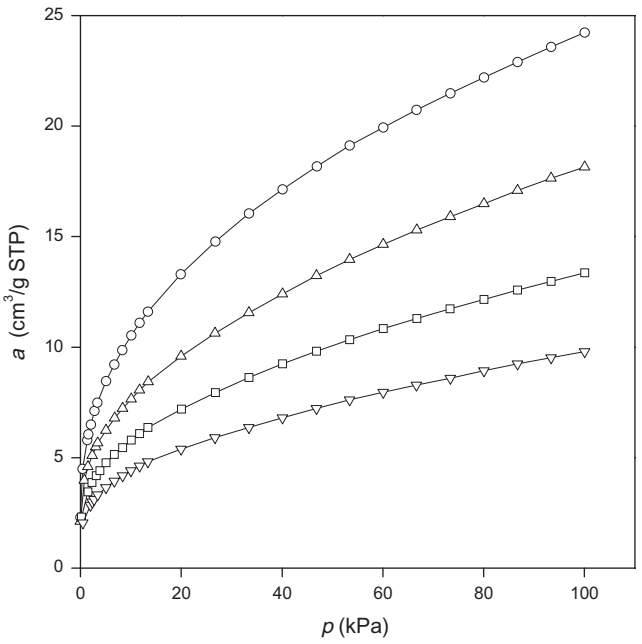

Fig. 8. Carbon dioxide isotherms on Mg/K-SBA-15 at 0 °C (○), 20 °C (△), 40 °C (□) and 60 °C (▽).

The interaction of CO_2 molecule with potassium cations gives rise to the pronounced increase in the isosteric heat of adsorption on sample Mg/K-SBA-15 attaining 46.5 kJ/mol for the small amount adsorbed. It is comparable with isosteric heats found for different alkali-metal exchanged low-silica zeolites being in the range from 40 to 50 kJ/mol [9,10].

Oliveira et al. [42] reported that in spite of the reduction of the surface area, hydrotalcites promoted by potassium yielded considerable improvements in adsorption capacity compared to those without potassium. It was suggested that a key factor for the CO_2 adsorption in the alkali-modified hydrotalcites was not attributable

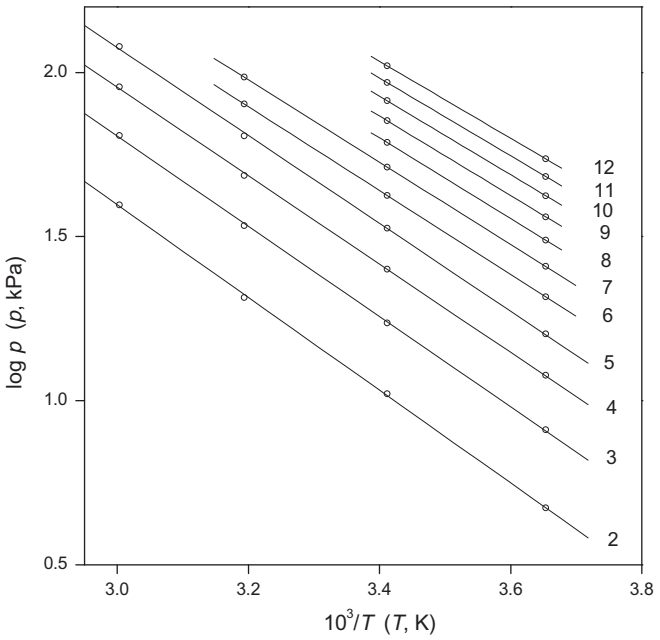

Fig. 9. Adsorption isosteres of carbon dioxide on sample Mg-SBA-15. Points were calculated by numerical interpolation (extrapolation) of adsorption isotherms, lines represent linear fit. All the isosteres are marked with corresponding amount adsorbed in cm/g STP.

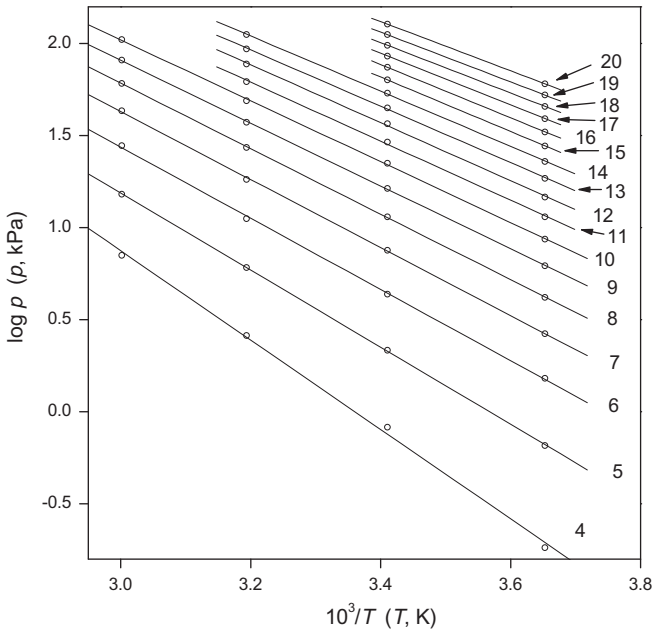

Fig. 10. Adsorption isosteres of carbon dioxide on sample Mg/K-SBA-15. Points were calculated by numerical interpolation (extrapolation) of adsorption isotherms, lines represent linear fit. All the isosteres are marked with corresponding amount adsorbed in cm^3/g STP.

to the surface area but to the presence of additional interactions with alkali cations. In the case of Mg/K-SBA-15, we have observed the same effect. Therefore, we can suppose that the sorption taking place on this adsorbent is a combination of physical adsorption and chemical reaction. In contrast to the hydrotalcite adsorbents, the structure of mesoporous silicas plays a crucial role. The structure of SBA-15 is obviously optimal for post-synthesis modification. Although the adsorption of CO_2 on pure SBA-15, SBA-16 and

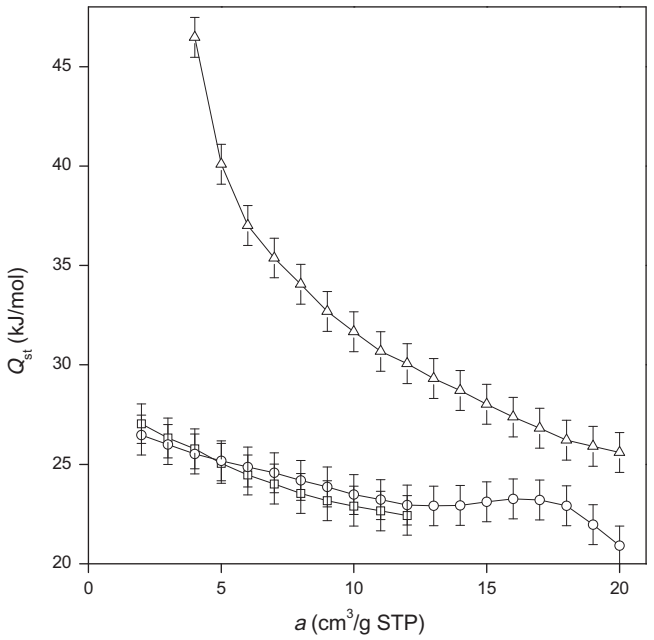

Fig. 11. Isosteric heats of adsorption of carbon dioxide on SBA-15 (○), Mg-SBA-15 (□) and Mg/K-SBA-15 (△). (The vertical bars denote assessed error of Q_{st} determination.)

MCM-48-ls silicas is similar, the described post-synthesis modification was successful only in the case of SBA-15.

4. Conclusions

A special method was developed in order to introduce magnesium oxide and potassium carbonate into the different structure types of mesoporous silica (SBA-15, SBA-16, MCM-48-ls) without a collapse of their porous systems. This procedure is based on the precipitation of magnesium acetate on the silica surface and its subsequent chemical conversion to magnesium oxalate, which decomposes directly to form magnesium oxide. To introduce potassium carbonate, MgO-modified silica was impregnated with potassium oxalate followed by conversion to carbonate.

It was shown that adsorption properties of prepared materials modified by magnesium oxide and promoted with potassium carbonate are decisively influenced by the type of mesoporous structure. The SBA-15 silica containing magnesium oxide and promoted by potassium carbonate exhibited the most steep adsorption isotherm. The CO_2 adsorption capacity of this sample was higher than that of analogous samples prepared from SBA-16 and MCM-48-ls silicas.

Acknowledgements

This work was supported by Grant Agency of the Czech Republic (project No. 203/08/0604). J.Č. would like to thank Visiting Professor Program, King Saud University, 378 Riyadh, Saudi Arabia.

Appendix A. Supplementary data

Supplementary data associated with this article can be found, in the online version, at http://dx.doi.org/10.1016/j.micromeso.2012.05.026.

References

[1] S. Choi, J.H. Drese, C.W. Jones, ChemSusChem 2 (2009) 796.
[2] N. Hedin, L.J. Chen, A. Laaksonem, Nanoscale 2 (2010) 1819.

[3] D.M. D'Alessandro, B. Smit, J.R. Long, Angew. Chem. Int. Ed. 49 (2010) 2.
[4] Q. Wang, J. Luo, Z. Zhong, A. Borgna, Energy Environ. Sci. 4 (2011) 42.
[5] F.N. Ridha, Y. Yang, P.A. Webley, Micropor. Mesopor. Mater. 117 (2009) 497.
[6] A. Ghoufi, L. Gaberova, J. Rouquerol, D. Vincent, P.L. Llewellyn, G. Maurin, Micropor. Mesopor. Mater. 119 (2009) 117.
[7] S.-T. Yang, J. Kim, W.-S. Ahn, Micropor. Mesopor. Mater. 135 (2010) 90.
[8] M. Palomino, A. Corma, F. Rey, S. Valencia, Langmuir 26 (2010) 1910.
[9] A. Pulido, P. Nachtigall, A. Zukal, I. Dominguez, J. Čejka, J. Phys. Chem. C 113 (2009) 2928.
[10] A. Zukal, A. Pulido, B. Gil, P. Nachtigall, O. Bludský, M. Rubeš, J. Čejka, Phys. Chem. Chem. Phys. 12 (2010) 6413.
[11] G.D. Pirngruber, P. Raybaud, Y. Belmabkhout, J. Čejka, A. Zukal, Phys. Chem. Chem. Phys. 12 (2010) 13534.
[12] A. Zukal, C.O. Arean, M.R. Delgado, P. Nachtigall, A. Pulido, J. Mayerová, J. Čejka, Micropor. Mesopor. Mater. 146 (2011) 97.
[13] P. Nachtigall, L. Grajciar, J. Pérez-Pariente, A.B. Pinar, A. Zukal, J. Čejka, Phys. Chem. Chem. Phys. 14 (2012) 1117.
[14] G.P. Knowles, J.V. Graham, S.W. Delaney, A.L. Chaffee, Fuel Process. Technol. 86 (2005) 1435.
[15] R.S. Franchi, P.J.E. Harlick, A. Sayari, Ind. Eng. Chem. Res. 44 (2005) 8007.
[16] C. Knöfel, J. Descarpentries, A. Benzaouia, V. Zeleňák, S. Mornet, P.L. Llewellyn, V. Hornebecq, Micropor. Mesopor. Mater. 99 (2007) 79.
[17] V. Zeleňák, D. Halamová, L. Gaberová, E. Bloch, P. Llewellyn, Micropor. Mesopor. Mater. 116 (2008) 358.
[18] V. Zeleňák, M. Badaničová, D. Halamová, J. Čejka, A. Zukal, N. Murafa, G. Goerigk, Chem. Eng. J. 144 (2008) 336.
[19] A. Zukal, I. Dominguez, J. Mayerová, J. Čejka, Langmuir 25 (2009) 10314.
[20] S. Choi, McM. L. Gray, C.W. Jones, ChemSusChem 4 (2011) 628.
[21] B. Aziz, G. Zhao, N. Hedin, Langmuir 27 (2011) 3822.
[22] A. Zukal, J. Jagiello, J. Mayerová, J. Čejka, Phys. Chem. Chem. Phys. 13 (2011) 15468.
[23] A. Zukal, J. Mayerová, J. Čejka, Phys. Chem. Chem. Phys. 12 (2010) 5240.
[24] Z Liang, M. Marshall, A.L. Chaffee, Energy Fuels 23 (2009) 2785.
[25] L. Hamon, E. Jolimaître, G.D. Pirngruber, Ind. Eng. Chem. Res. 49 (2010) 7497.
[26] G. Férey, C. Serre, T. Devic, G. Maurin, H. Jobic, P.L. Llewellyn, G. De Weireld, A. Vimont, M. Daturi, J.-S. Chang, Chem. Soc. Rev. 40 (2011) 550.
[27] M. Badaničová, V. Zeleňák, Monatsh. Chem. 141 (2010) 677.
[28] S. Bourrelly, P.L. Llewellyn, C. Serre, F. Millange, T. Loiseau, G. Férey, J. Am. Chem. Soc. 127 (2005) 13519.
[29] N.A. Ramsahye, G. Maurin, S. Bourrelly, P. Llewellyn, T. Loiseau, G. Ferey, Phys. Chem. Chem. Phys. 9 (2007) 1059.
[30] J. Roggenbuck, M. Tiemann, J. Am. Chem. Soc. 127 (2005) 1096.
[31] J. Roggenbuck, G. Koch, M. Tiemann, Chem. Mater. 18 (2006) 4151.
[32] S.-W. Bian, J. Baltrusaitis, P. Galhotra, V.H. Grassian, J. Mater. Chem. 20 (2010) 8705.
[33] A. Zukal, H. Šiklová, J. Čejka, Langmuir 24 (2008) 9837.
[34] T.-W. Kim, R. Ryoo, M. Kruk, K.P. Gierszal, M. Jaroniec, S. Kamiya, O. Terasaki, J. Phys. Chem. B 108 (2004) 11480.
[35] T.-W. Kim, F. Kleitz, B. Paul, R. Ryoo, J. Am. Chem. Soc. 127 (2005) 7601.
[36] H. Yan, C.F. Blanford, B.T. Holland, W.H. Smyrl, A. Stein, Chem. Mater. 12 (2000) 1134.
[37] C.-H. Yang, B. Zibrowius, W. Schmidt, F. Schüth, Chem. Mater. 16 (2004) 2918.
[38] A.A. Gurinov, Yu.A. Rozhkova, A. Zukal, J. Čejka, I.G. Shenderovich, Langmuir 27 (2011) 12115.
[39] D. Nachtigallová, O. Bludský, C.O. Areán, R. Bulánek, P. Nachtigall, Phys. Chem. Chem. Phys. 8 (2006) 4849.
[40] P. Nachtigall, M.R. Delgado, D. Nachtigallova, C.O. Arean, Phys. Chem. Chem. Phys. 14 (2012) 1552.
[41] S.C. Lee, H.J. Chae, S.J. Lee, B.Y. Choi, C.K. Yi, J.B. Lee, J.C. Kim, Environ. Sci. Technol. 42 (2008) 2736.
[42] E.L.G. Oliveira, C.A. Grande, A.E. Rodrigues, Sep. Purif. Technol. 62 (2008) 137.